Biomatter 4, e27993; February; © 2014 Landes Bioscience

Comprehensive histological evaluation of bone implants

Claudia Rentsch[1,2,*], Wolfgang Schneiders[1], Suzanne Manthey[1,2], Barbe Rentsch[2], and Stefan Rammelt[1,2]

[1]Department of Trauma and Reconstructive Surgery; University Hospital Carl Gustav Carus; Technische Universität Dresden; Dresden, Germany; Dresden, Germany;
[2]University Hospital and Medical Faculty; Technische Universität Dresden; Centre for Translational Bone, Joint and Soft Tissue Research; Dresden, Germany

Keywords: bone implants, polycaprolactone-co-lactide scaffold, sheep, histology

To investigate and assess bone regeneration in sheep in combination with new implant materials classical histological staining methods as well as immunohistochemistry may provide additional information to standard radiographs or computer tomography. Available published data of bone defect regenerations in sheep often present none or sparely labeled histological images. Repeatedly, the exact location of the sample remains unclear, detail enlargements are missing and the labeling of different tissues or cells is absent. The aim of this article is to present an overview of sample preparation, staining methods and their benefits as well as a detailed histological description of bone regeneration in the sheep tibia. General histological staining methods like hematoxylin and eosin, Masson-Goldner trichrome, Movat's pentachrome and alcian blue were used to define new bone formation within a sheep tibia critical size defect containing a polycaprolactone-co-lactide (PCL) scaffold implanted for 3 months (n = 4). Special attention was drawn to describe the bone healing patterns down to cell level. Additionally one histological quantification method and immunohistochemical staining methods are described.

Introduction

The biology of fracture healing is a complex biological process that follows a specific regenerative pattern and involves changes of the gene expression level. Bone rebuilds by either direct intramembranous (primary) or indirect (secondary) fracture healing. Indirect fracture healing consists of both intramembranous and endochondral bone formation and can be seen in large defects after operative fracture treatment, presenting weight bearing and thereby micro motion.[1]

Secondary bone repair occurs in 4 overlapping stages:

Stage I

The first stage, the initial inflammatory response, includes formation of the hematoma, inflammation and the recruitment of mesenchymal stem cells (MSC) as biological process.

Stage II

The second stage, the soft callus formation, encompasses chondrogenesis, endochondral and intramembraneous ossification and angiogenesis. MSC are recruited in order to differentiate into chondrogenic and osteogenic line. Cells like chondroblasts, chondrocytes, chodroclasts as well as osteoblasts, osteocytes and osteoclasts are essential for the bone forming progression.

MSC can differentiate into chondroblasts and produce collagen type II and proteoglycans to establish mechanical stability. Finally, cartilage undergoes hypertrophy and controlled mineralization. Chondroclasts remove the cartilage as soon as vessels invade so that woven bone formation can occur by MSC which underwent osteogenic differentiation. Osteoblasts synthesize a new collagenous organic matrix and regulate the mineralization. When embedded in the newly produced matrix osteoblasts become osteocytes. Osteocytes develop a fine filopodia network to remain in cell-cell contact. Osteoclasts, derived from mononuclear precursors, can bind to bone matrix peptides via integrin receptors and resorb the matrix.

The organic extracellular matrix (ECM) is composed of collagens, glycoproteins, hyaluronic acid and proteoglycans. The ECM provides the structural scaffold for cells, growth factors and cytokines.

A three dimensional vascular network is formed in the bone defect by invading endothelial cells, smooth muscle cells, and pericytes.

Stage III

The third stage, the hard callus formation, is defined by osteogenesis, including bone cell recruitment and woven bone formation that takes place after chondrocyte apoptosis, chondroclast recruitment and cartilage resorption in the soft callus.

Stage IV

Stage four, bone remodeling, involves osteoblast, osteoclast and endothelial cell activity with resorption of the woven bone and formation of cortical and trabecular bone.[1-3]

Current clinical options in the treatment of large bone defects pose a continuous challenge in orthopedic surgery. Although currently available data provide complex information on bone

*Correspondence to: Claudia Rentsch; Email: claudia.rentsch@uniklinikum-dresden.de
Submitted: 10/14/2013; Revised: 01/13/2014; Accepted: 01/24/2014; Published Online: 02/06/2014
Citation: Rentsch C, Schneiders W, Manthey S, Rentsch B, Rammelt S. Comprehensive histological evaluation of bone implants. Biomatter 2014; 4:e27993; PMID: 24504113; http://dx.doi.org/10.4161/biom.27993

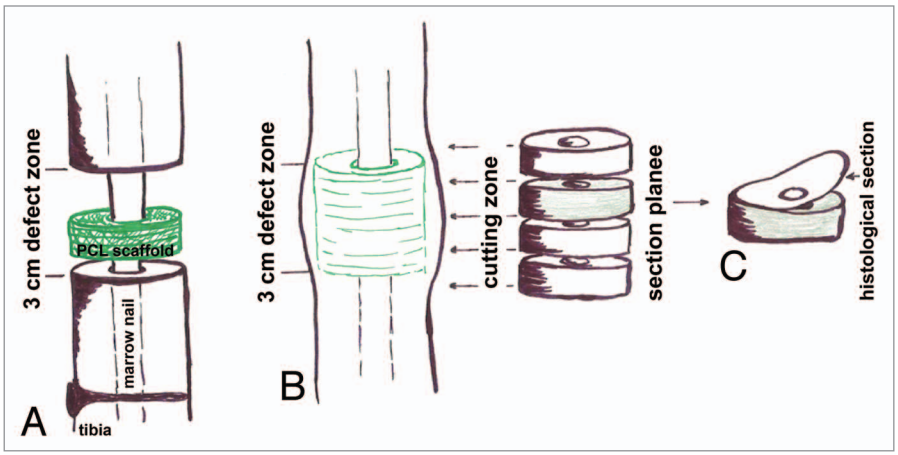

Figure 1. Schematically drawing of sample preparation for histological investigations. (**A**) Sheep tibia defect stabilized by a marrow nail, beginning PCL scaffold implantation to fill the defect. (**B**) Callus formation within the defect zone after 3 mo of implantation, for histological/immunohistological evaluations sections through the whole defect zone were created. (**C**) Histological sections (3 µm) of each plane were used for all staining's (HE, Masson-Goldner trichrome, modified Masson-Goldner trichrome, alcian blue, 1A4-Actin, osteopontin).

healing pathways, many open questions remain. To enhance fracture healing in critical bone defects different biomaterials, like hydroxyaptite, polymers, metals and composites[4-6] have been proposed, but until now most of them are not incorporated into the clinical setting.[7-9]

The use of animal models has made it possible to investigate fracture healing in general and in addition with new implant materials. Histologically, the bone structure of younger sheep (age 1–4) is quite different (laminar cortical bone) compared with the secondary human bone structure. To investigate human like bone remodeling sheep with an age of 7–9 (which present secondary (osteonal) remodeling) have to be used.[10]

However, histological investigations about detailed healing stages in sheep large bone defects and the analysis of the partial distribution of the cells with respect to the biomaterials are rare. Most presented histological figures of defect areas describe only the presence or absence of the implant material and bone.[11-15] Frequently, the location of the token picture within the defect area remains unclear, detail enlargements are missing and the labeling of different tissues or cells are simple or absent.[16-21] More specific labeled histological images about cells and tissue can be found in the publications of Claes et al., Mastrogiacomo et al., Niemeyer et al., Gao et al., Marcacci et al., and Reichert et al. but some information is always missing.[22-27] Informative detailed histological studies and images, with exhaustive evaluations, are presented for example by Lohfeld et al., Harms et al., and Liu et al.[28-30]

This investigation established general histological staining methods on ovine bone as a large animal model for bone healing studies. It has to be considered that this publication describes the investigation of a polymeric, porous implant and offers thereby a partial view of a complex histological issue. Different methodical problems can be encountered when processing other types of materials. Bones containing hard materials as metallic or ceramic implants have to undergo the cutting and grinding technique since they can't be sectioned by a microtome. Metallic implants like screws could be removed before decalcification but usually not without small damages of the surrounding tissue, especially at the bone-biomaterial interface. Ceramic implants (e.g., calcium phosphate, hydroxyapatite, alumina, zirconia, and bioglasses) are not suitable to decalcification.

The aim of this study was to describe histological slides in detail to identify the bone healing patterns down to the cell level. A classification of cell and tissue type within the defect area, the state of bone healing, the performance of the implant material, the status of inflammation and vascularization was considered to evaluate the staining method as well as the healing process. The intention is to provide one concept for the description of the image location as well as detailed image labeling and to encourage scientists to plan and describe their explant sample preparation for bone histology at full-length. To achieve this goal a biomaterial (polycaprolactone-co-lactide [PCL]) was implanted in a sheep (age 6–9) tibia critical size defect (n = 4) for 3 mo.

This presentation will support the histological understanding of sectional images relating to new bone formation on new implant materials.

Results and Discussion

Histological evaluation

New bone formation was detected with all histological staining methods at the proximal and distal ends of the 3 cm defect zone. The new bone was mainly localized in the external scaffold area. The new bone matrix enclosed the scaffold fibers without any connective tissue interface. No inflammatory reaction was visible around the implant material after 3 mo.

HE staining

HE staining allowed a general overview of the histological section. Bone was presented as a compact structure in a dark red color. The connective tissue is more displayed as a structured network of cells and collagen fibers in a lightly pink color (**Fig. 2**). Cartilage appears in a gray-pink mix but all tissues have to be

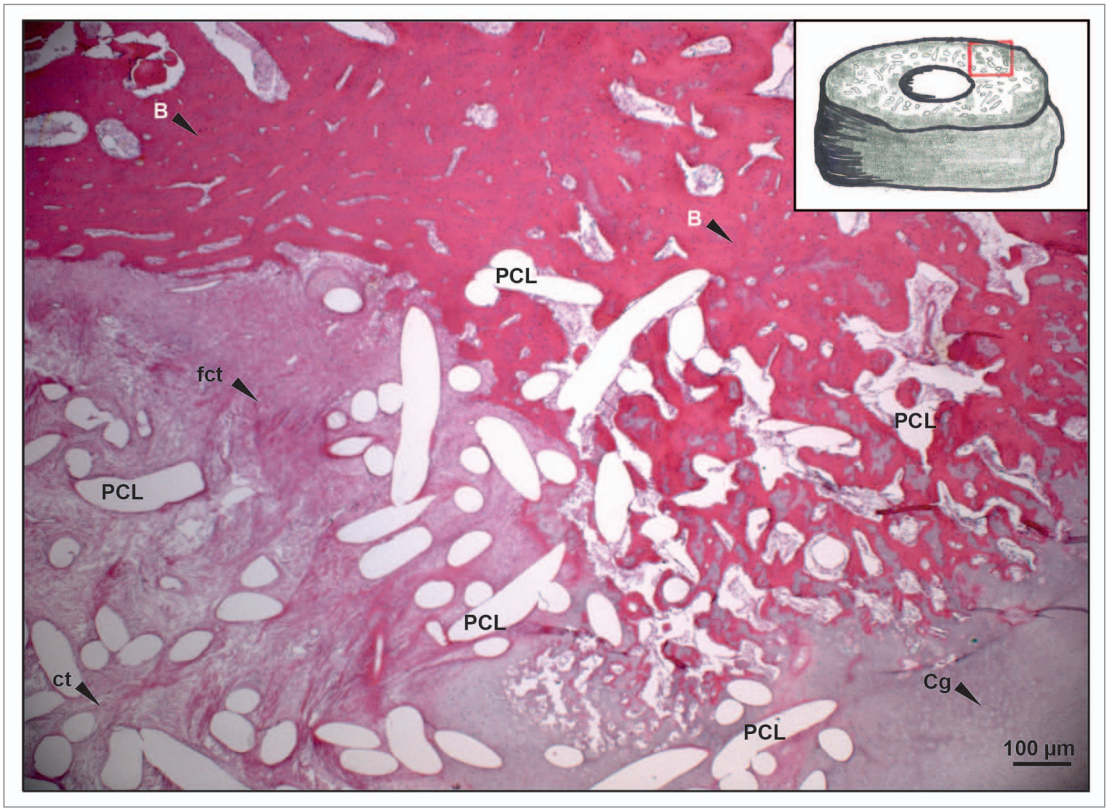

Figure 2. HE staining overview. Bone is presented as a compact structure in a dark red color, connective tissue in light pink and the porous scaffold structure (PCL) in white. Areas of direct ossification present structures of firm connective tissue showing positioned collagen fibers. The drawing at the right top corner provides the orientation of the presented image (red frame). (original magnification 100x). B, Bone; Cg, cartilage; fct, firm connective tissue; ct, connective tissue.

morphological separated. The PCL scaffold material has been dissolved during the process of depolymerization. Therefore, the white spots in the histological sections present the original implant material. The amount of new calcified bone in the defect area as well as inside of the porous implant can be easily estimated by HE staining.

Thorough analyses of histological sections allow far more detailed information about bone healing status and the function of the implant material. Different cell types and tissues can be determined by different histological staining methods like HE, Masson-Goldner trichrome, modified Masson-Goldner trichrome, Movat's pentachrome or alcian blue staining.

HE staining allowed different cell type localization only through morphological structure identification (**Fig. 3**). Osteocytes, osteoblast and chondrocytes could be distinguished in the hard tissue components whereas fibroblasts were located within the connective tissue. Areas of direct ossification (do) presented as structures of firm connective tissue showing positioned, tightly packed, large collagen fibers with less fibroblasts compared with regular connective tissue (**Fig. 3**, [do] yellow arrow). Regions of cartilage formation could be detected in all histological section planes of the 3 cm defect area indicating endochondral ossification (eo) (**Fig. 3**, [eo] yellow arrow). Signals of chronic inflammation (macrophages, foreign body giant cells or neutrophils could not be detected after 3 mo.

Masson-Goldner trichrome staining

Masson-Goldner trichrome staining is a commonly used method in bone histology and allows tissue identification by different coloring as well as by morphological identification.

In this investigation bone structures of the new build callus tissue were shown in a compact green color. The newly formed lamellar bone inside the scaffolds presented osteons including Haversian canals (see orange circle in **Fig. 4A-C**). The average diameter varied between 100 and 400 µm (**Fig. 4C**) and the number of lamellae ranged between 4 and 20 (**Fig. 4D**). Collagen fibrils are arranged in a helical order. The canals measured between 20–50 µm and contained up to 3 blood vessels which were surrounded by connective tissue (**Fig. 4D**). The detection of Haversian canals within the newly formed bone inside the scaffold indicates a regular bone formation. The presence of vessels can be certainly detected when erythrocytes are seen that appear in a bright pink color (**Fig. 4C**).

According to their physiological localization, osteocytes and osteoblasts can be localized within the newly formed bone and at the margin of the trabeculae as lining cells respectively. Osteoclasts or chondroclasts can be visualized as polynucleated cells which appear in a red-brown color. The finding of osteoblasts and osteoclasts indicate a regulated process of bone formation and resorption. These findings indicate that after 3 mo of

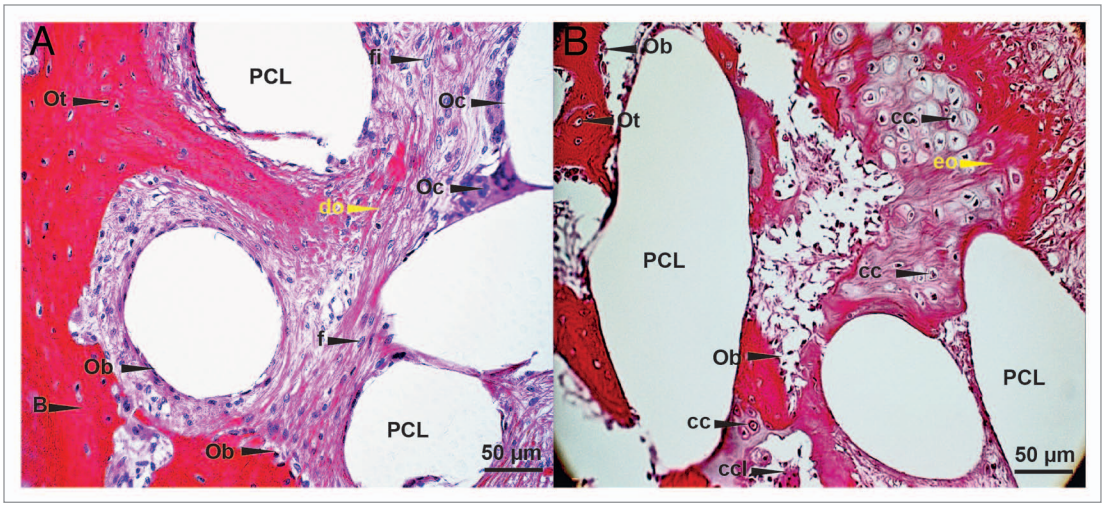

Figure 3. HE staining – detailed investigation. (**A and B**) Bone is presented as a compact structure in a dark red color, connective tissue in light pink and the porous scaffold structure (PCL) in white. (original magnification 200x). Ob, osteoblast; Oc, osteoclast; Ot, osteocyte; fi, fibroblast; bv, blood vessel; rl, resorpition lacuna; Cg, cartilage; mL, chondrocyte; ccl, chondroclast; do, direct ossification; eo, endochondral ossification.

scaffold implantation the second and third stage of bone healing can be observed.

Radiographic measurements may provide information about the amount of new bone formation within the defect area but often there is no information about the presence and state of the implant material or the conditions of non calcified tissue. The quantification of an adequate amount of histological images is time consuming and complicated but one option of area quantification will be presented here. First of all a modification of a standard staining method had to be done to allow a distinct separation of the different tissues to permit a defined threshold measurement for computer analysis.

Modified Masson-Goldner trichrome staining

The modified Masson-Goldner trichrome staining (**Fig. 5A and B**) allowed a clear separation of connective tissue (dark green) and bone matrix (yellow). Small islets of bony matrix at the inner parts of the scaffold straight around the scaffold fibers were detected indicating an osteogenic differentiation of the connective tissue cells (**Fig. 5B**). The histological identification of single cells was more difficult because of the intense coloring.

The quantification of new bone formation within the scaffold, the amount of connective tissue as well as the remaining PCL material was possible using the imaging software "cell^{D}" (**Fig. 5C and D**).

On average, 44% new bone, 9% PCL material and 48% connective tissue was seen in the defect area using histological coloring for quantitative measurements. The measurements correlated with additionally conducted micro-computer tomography showing 51% new bone formation on average (data not shown).

Movat's pentachrome staining

The Movat's pentachrome staining presented one of the best coloring methods for detailed analysis of bone healing progressions. Mature bone is shown in a compact structure in dark yellow compared with fibrous tissue in light yellow and cartilage tissue in green (**Fig. 6A and B**). New formed osteoids are colored in red (**Fig. 6C**, top left). The active stage of new bone accumulation within the scaffold can be seen in **Figure 6C** (red staining). The maturing bone structures are clearly visible but they don't show a well-organized osteonic structure yet.

The strong contrast between the yellow collagen fibers and the brown nuclei staining allowed a clear and comfortable identification of the existing cells and matrix. Osteoblasts, osteocytes and osteoids could be analyzed similar to the Masson-Goldner trichrome staining (**Fig. 6A and B**).

The formation of new collagen fibers is crucial for the estimation of intramembranous ossification (direct new bone formation). Collagen producing fibroblasts transport the collagen molecule into the extracellular space where they polymerize to larger fibrils. Casual fibrous tissue has small collagen and elastic fibers. Firm connective tissue presents with tightly packed collagen clusters in different directions (see violet labeling in **Fig. 6D**). Increasing production of collagen matrix is directed by the differentiating fibroblasts which take over an osteoblast-like function. During direct new bone formation the developing osteoblast transforms into an osteocyte within the collagen matrix.

Alcian blue staining

Endochondral ossification was visualized with alcian blue staining (**Fig. 7**), labeling glycosaminoglycans in a bright blue color. The chondrocytes were clearly detectable within the hyaline cartilage structure and formed chondrones (**Fig. 7**). The dark blue coloring around the chondrones indicates a matrix rich in highly sulfated glycoseaminoglycans. In close proximity to the bone, a process of diverse remodeling was observed, consisting of loose and firm connective tissue and cartilage. **Figure 7** represents a characteristic area of new bone formation in the PCL scaffold, with distinct areas marked showing cartilage and bone formation. The dark blue staining represents vesicular cartilage that produces calcified matrix and dying chondrocytes. Chondroclasts remove the matrix and ingrowing mesenchymal tissue incorporates vessels and osteoprogenitor cells which differentiate into

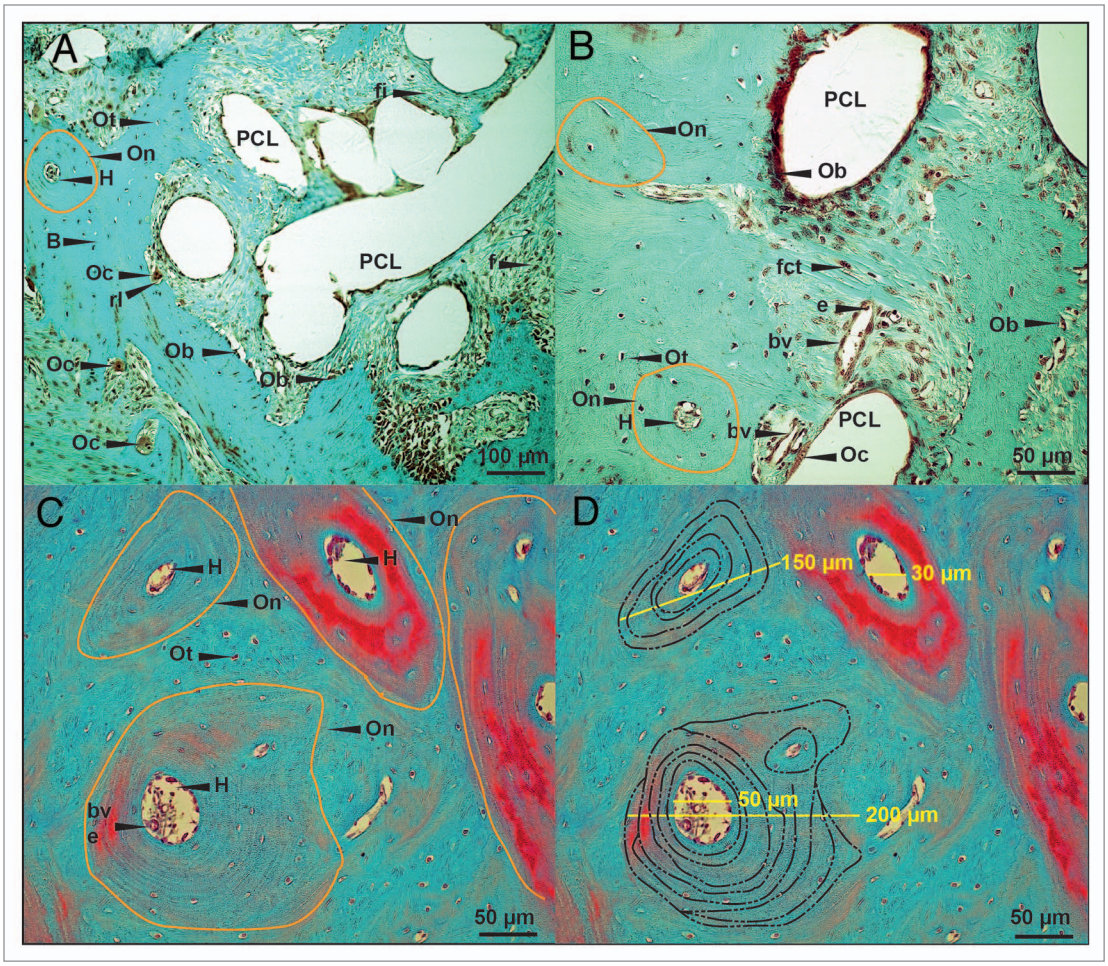

Figure 4. Masson-Goldner trichrome staining – detailed investigation. (**A and B**) Detailed description of new bone formation within the PCL scaffold. (**C and D**) Identical images presenting osteons in general (**C**, orange line) as well as measuring bars to describe the osteon size and the number of lamellae (**D**); (original magnification: **A**, 100x; **B and D**, 200x). Ob, osteoblast; Oc, osteoclast; Ot, osteocyte; On, osteon (orange); H, Haversian canal; fi, fibroblast; bv, blood vessel; rl, resorpition lacuna; e, erythrocyte; fct, firm connective tissue; black dashed line, lamellae; yellow bars, measuring of H or On.

osteoblast and form bone matrix. **Figure** 7 shows chondrocytes and their chondrones as well as matrix removing chondroclasts in the endochondral ossification area. Additionally, intramembranous ossification is present, as well as fibroblasts, which produce a collagen matrix and firm connective tissue. Ingrowing progenitor cells differentiate into osteoblasts and produce calcified bone matrix.

Table 1 provides an overview of the staining methods used in our study, the detected tissues and structures and finally the suggested application.

Immunochemical evaluation

Anti- α smooth muscle actin staining

Anti-α smooth muscle actin (1A4) staining was used to mark smooth muscle cells in vessel walls. Actins are highly conserved proteins that are involved in various types of cell motility and are ubiquitously expressed in all eukaryotic cells. The human antibody allowed a good cross reaction with ovine tissue and a specific detection of vessels.

A complete vascularization was observed in all sections of all animals. Vascularization occurred throughout the entire 3 dimensional scaffold stack and included vessels ranging from 0.1 to 1 mm in diameter (**Fig. 8A**).

Osteopontin

Osteopontin is a secreted, highly acidic, calcium binding, phosphorylated glycoprotein that is chemotactic for macrophages, smooth muscle cells, endothelial cells, and glial cells. Osteopontin binds over integrin, using an RGD signal, on cell surfaces. To interact with the ECM it can also bind on collagen I. The human antibody also permitted a specific cross reaction with ovine tissue.

Positive osteopontin staining (**Fig. 8B**, brown color) was evident at the firm connective tissue areas around the scaffold fibers as well as at the osteoblasts near the bone-connective tissue border. The high resolution picture in **Figure 8 B** shows osteopontin clearly associated within the collagen fibers.

Summary

All presented staining methods (HE, Masson-Goldner trichrome, modified Masson-Goldner trichrome, Movat's pentachrome and alcian blue staining) can be used to identify new bone formation within a porous polymeric implant. However,

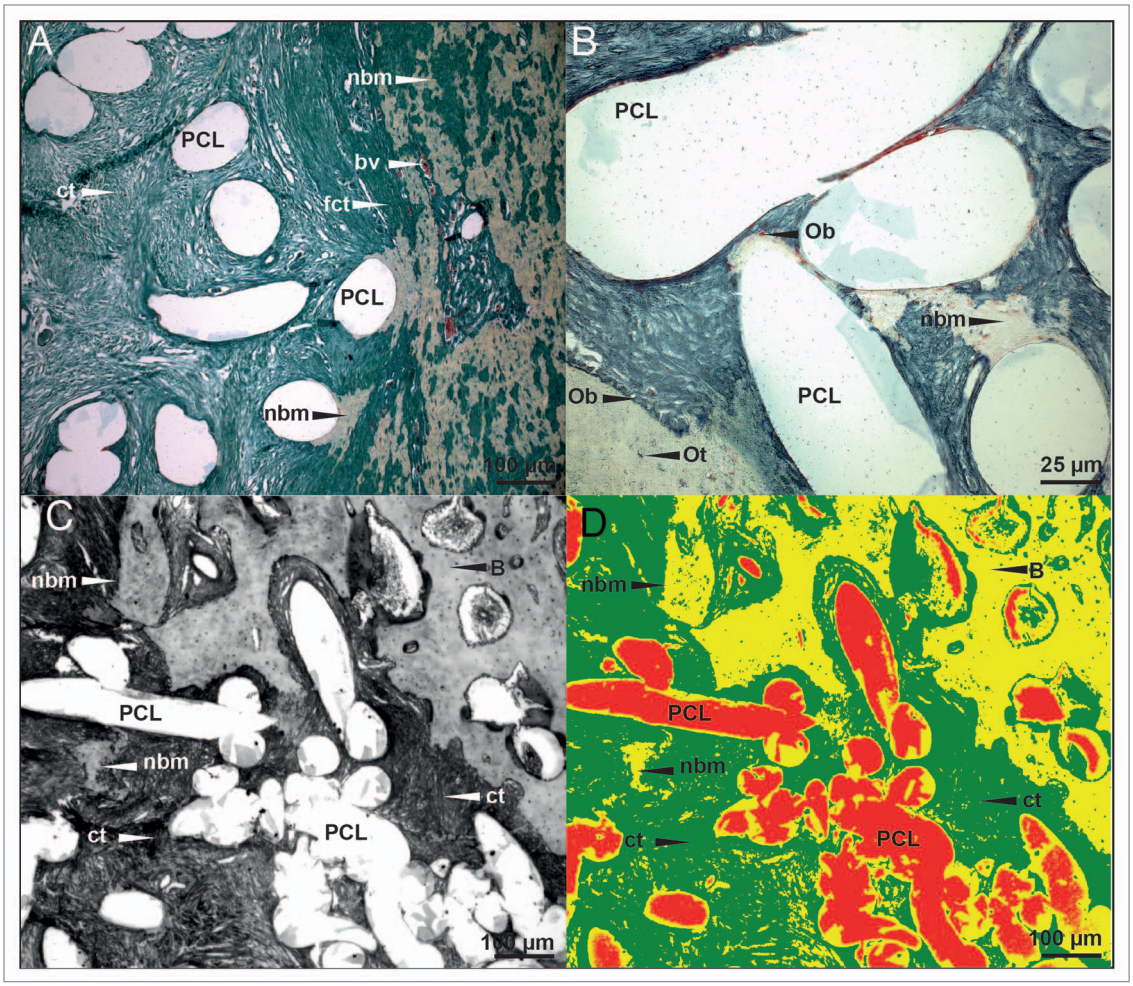

Figure 5. Modified Masson-Goldner trichrome staining: detailed investigation. (**A**) Modified Masson-Goldner trichrome, (**B**) detailed description, (**C**) original image for histological quantification using false coloring, (**D**) false coloring of image C using Olympus software "cell^{D}". Connective tissue in green (45%), bone in yellow (35%) and PCL fiber in red (20%); (original magnification: **A, C, and D**, 100x; **B**, 400x). Ob, osteoblast; Ot, osteocyte; bv, blood vessel; nmb, new bone matrix; fct, firm connective tissue; ct, connective tissue.

they allow far more detailed information about the bone healing status and present cell types.

After 3 mo of PCL coll I/cs scaffold implantation in a critical size tibia defect all histological sections represented the second stage of the fracture healing according to Schindler et al.[2] The scaffold was completely intermingled with vascularized, connective tissue (**Figs. 4 and 8A**), showing small bony islets around the PCL fibers at the inner part of the scaffold (**Figs. 5 and 6**), and intermediate states of bone formation (**Figs. 2–6**).

A general overview about implant material and new bone formation was given by HE and Masson-Goldener trichrome staining.

Modified Masson-Goldener trichrome staining allowed a distinct coloring between connective tissue, new bone formation and the dissolved implant material and could be used for quantitative measurements (**Fig. 5**). This coloring method has to be adjusted for other implant materials since other scaffolds might react differently during histological preparation.

In this investigation, the Movat's pentachrome staining method provided the most distinct coloration between cartilage, mature bone, connective tissue new osteoids and cell nuclei. This staining method was optimal for the detection of intramembranous and / or endochondral ossification since cell (nuclei) and collagen fiber aggregation were considered as well as cartilage formation and/or new bone formation. Reichert et al. also used Movat's pentachrome to describe the morphology of newly formed bone in polycaprolactone and tricalcium phosphate combined scaffolds in sheep defects. New osteoids, blood vessels, osteoblast and osteoclasts were detected and labeled in these sections.[27]

Glucosaminoglycans and their producing chondroblasts and chondrocytes were clearly labeled by alcian blue staining (**Fig. 7**). Endochondal ossification (soft callus remodeling) represents a typical fracture healing stage according to the four stage model.[2] Multinucleated cells within the soft callus as well as at the new woven bone were detected. Based on the physical location of multinucleated cells, they are termed chondroclasts for cartilage and

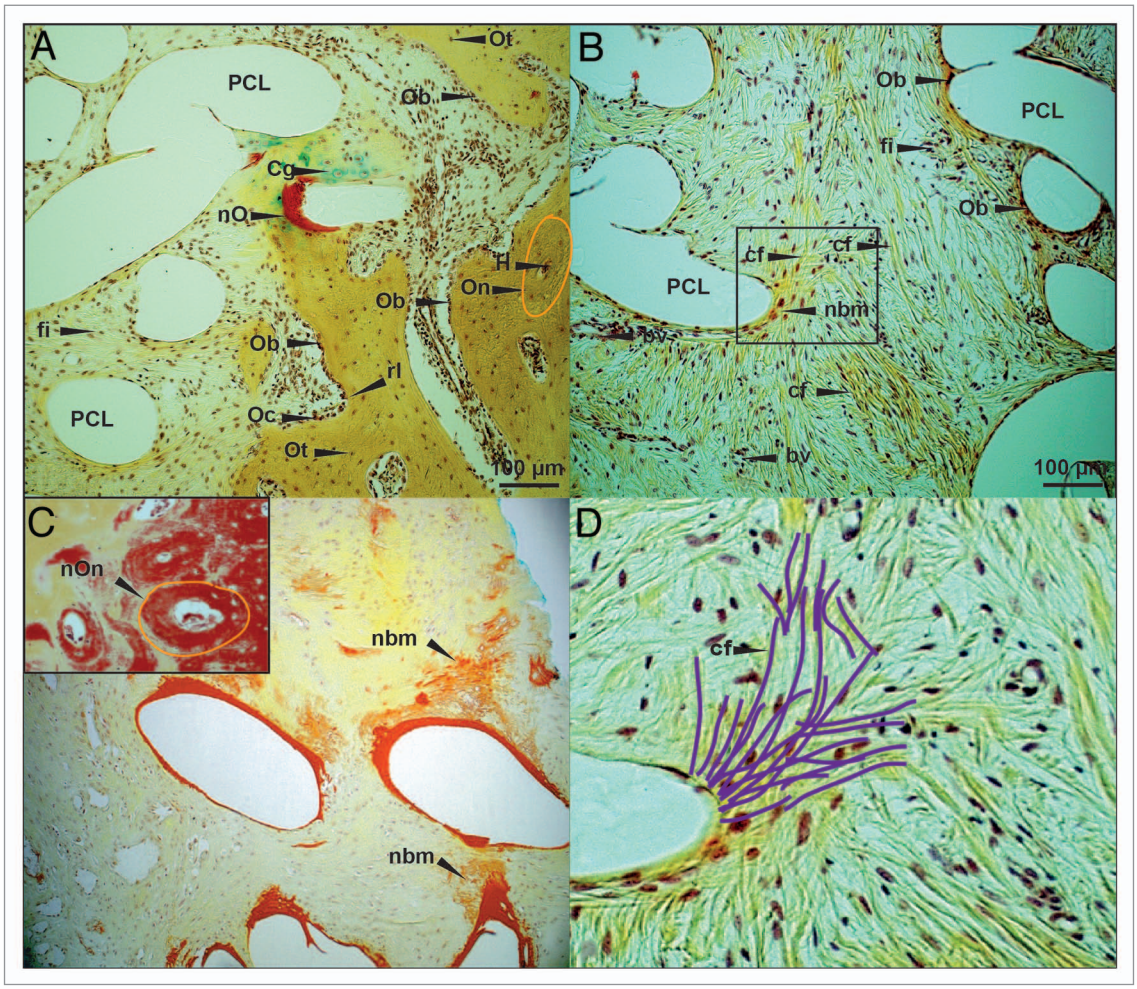

Figure 6. Movat's pentachrome staining: detailed investigation. (**A and B**) Detailed description of new bone formation within the PCL scaffold. (**C**) Active stage of new bone accumulation, left top picture shows well organized new osteons. (**D**) Enlargement of (**B**) (black frame) presenting detailed collagen structure, partly marked with violet lines; (original magnification: **A and B**, 100x). Ob, osteoblast; Oc, osteoclast; Ot, osteocyte; H, Haversian canal; On, osteon (red circle); fi, fibroblast; bv, blood vessel; rl, resorpition lacuna; nmb, new bone matrix; nO, new osteoids; Cg, cartilage; cf, collagen fibers.

osteoclasts for bone.[2] According to the callus remodeling system of Schindler et al. chondroclasts are the main effectors in cartilage resorption followed by endothelial cells for new vascularization and bone formation.[2]

Additionally, a high osteogenic activity at the bone-connective tissue interface was evident by osteopontin staining, indicating intramembranous ossification. Osteoblasts and their progenitor cells are clearly stained by osteopontin (**Fig. 8B**, dark brown). Connective tissue invaded precursor cells (brown) showed a high osteogenic activity as well. Osteopontin is expressed by osteocytes, osteoblast and their precursors as well as by osteoclasts and hypertrophic chondrocytes.[31] It is assumed to be a multifunctional protein that is involved in bone turnover and remodeling activities.

Conclusion

Standard histological staining methods on ex vivo samples can provide more information than there is bone or none. This study has demonstrated that different histological stains at explanted PCL bone implants approve individual qualities of information about tissue types, single cell types, the state of bone healing, the performance of the implant material, the status of inflammation and vascularization. Being familiar with the morphology of bone tissue and implant behavior a basic HE staining provides decent information. To achieve quantification options of single cells, special tissue areas or remaining implant materials more complex staining methods (like Masson-Goldner trichrome, modified Masson-Goldner trichrome, Movat's pentachrome) should be investigated. Regarding the actual results the authors recommend Movat's pentachrome staing for the analysis of the new growing tissue within the implant.

As a resume: Histology is a time consuming method but it provides excellent details in bone healing. Histology, radiographs and CT images can complement each other, giving different information and at different levels of investigation. Taken the time to describe sample preparation, the location of the presented

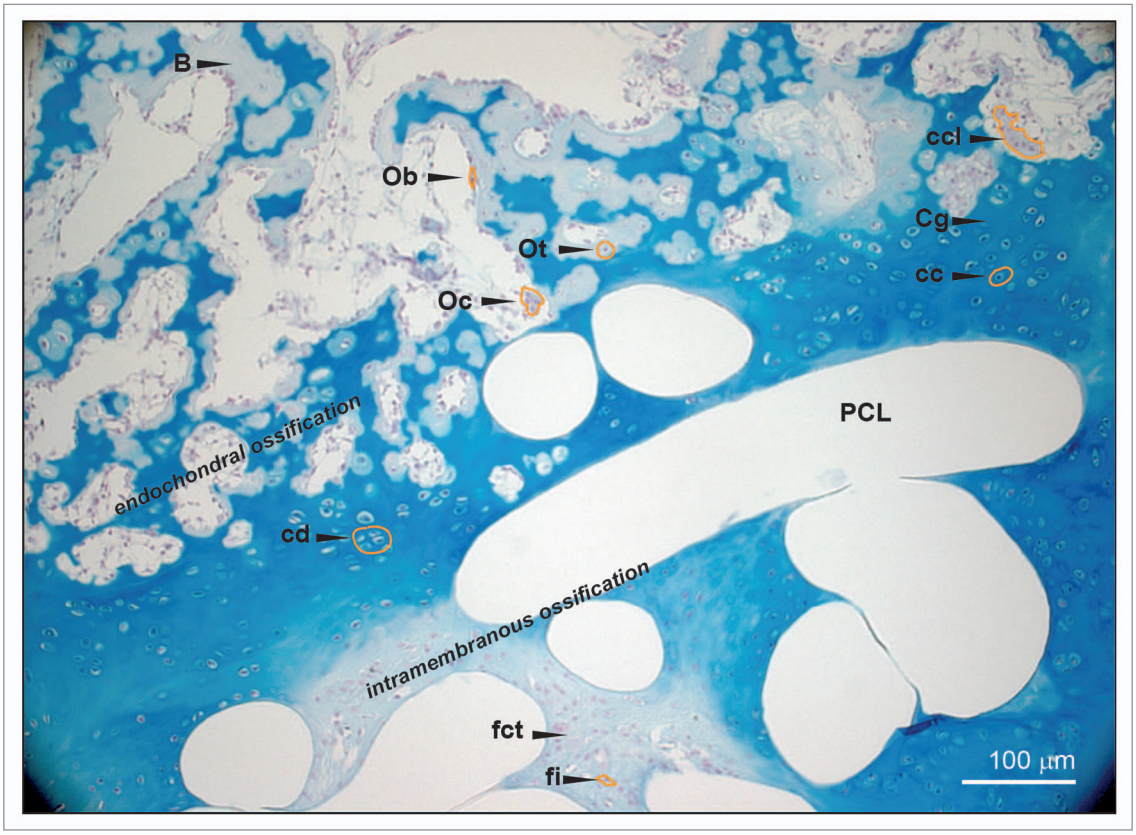

Figure 7. Alcian blue staining. Morphological identification of different cell types (orange circles) and ossification areas (endochondral or intramembranous) within the scaffold. (original magnification 100x). Ob, osteoblast; Oc, osteoclast; Ot, osteocyte; B, bone; fi, fibroblast; fct, firm connective tissue; Cg, cartilage; mL, chondrocyte; ccl, chondroclast; cd, chondrone.

Table 1. Final summary

Staining method	Described color results	Identifiable tissues and structures	Suggested application
HE	Nuclei: blue Eosinophilic structures: pink	Bone: dark pink Connective tissue: light pink Vessel containing erythrocytes: bright red Nuclei: blue	General overview
Masson-Goldner trichrome	Nuclei: brown, black Cytoplasm: red Erythrocytes: orange Collagen: green	Bone: green, turquois Connective tissue: light green Vessel containing erythrocytes: pink Nuclei: brown	General overview
Modified Masson-Goldner trichrome	Nuclei: brown, black Cytoplasm: red Erythrocytes: orange Collagen: yellow-green	Bone: beige/yellow Connective tissue: dark green Vessel containing erythrocytes: orange	Distinct separation of connective tissue and bone matrix for quantification
Movat's pentachrome	Nuclei and elastic fibers: brown Cartilage: green Collagen: yellow New osteoids: red	Bone: dark yellow Connective tissue: light yellow Cartilage: green New osteoid: red Nuclei: brown	Optimal for detection of intramembranous and/or endochondral ossification
Alcian blue	Acid mucopolysaccharides and Glycosaminoglycans: blue Nuclei: red-brown	Cartilage: dark blue Connective tissue: gray/light blue Bone: gray Nuclei: red-brown	Optimal for detection of endochondral ossification

image and a detailed labeling of images, histology can improve information.

Material and Methods

PCL scaffold and coating

The textile polycaprolactone-co-lactide (Catgut GmbH, Markneukirchen, trade name: PCL) scaffolds with 19 mm external diameter were made on a computer aided embroidery machine. Scaffolds were coated with collagen type I and chondroitinsulfate (coll I/cs) like previously described.[32] To create a 3 cm high, three dimensional implant, 30 single scaffold disks were piled up. The scaffold stack showed homogeneously distributed interconnected porosity of 87% and a main pore size range of 0.1–0.8 mm.[32]

Surgical procedure

The study has been licensed by the regional board (24D-9168.11-1-2006-17), all animals were cared for according to the European guidelines for the care and use of laboratory animals (Directive 24.11.1986, 86/609/CEE).

Female sheep (n = 4) with an average body weight of 65 kg and an age of 6–9 y were used for this study. Surgery was performed like previously described.[33]

A 3 cm long segmental mid-diaphyseal osteotomy was performed on the left tibia of each sheep. The tibia was stabilized by a prototype unreamed tibial nail (UTN, Clinical House GmbH). The 3 cm resected bone segment, including its periosteum, was removed. The defect was filled with surface coated coll I/cs scaffolds for 3 mo.

Histology/immunohistology

Explants were fixed in 4% neutral buffered formalin (SAV LP) for at least 7 d (**Fig. S1**). The samples were washed, decalcified for 4 wk in EDTA (OSTEOSOFT, Merck KGaA, Darmstadt, Germany; to adjust pH to 7.4–7.6 use NaOH) using a automated microwave based tissue Processor RHS-1 (Diapath S.p.A,), dehydrated overnight in a Thermo Scientific STP 420*ES* Tissue Processor (Microm International GmbH, Part of Thermo Fisher Scientific), and embedded in methyl methacrylate (Technovit 9100 New, Heraeus Kulzer GmbH

The defect area was localized by measuring the distance between proximal and distal locking screw and the visible callus formation. The defect zone was cut in 7 equal section planes of 0.5 cm, beginning and ending beyond the implant area (**Fig. 1B**). Sections of 3 µm of each section plane (**Fig. 1C**) were prepared (rotation microtome RM2055, Leica Microsystems) and methyl-methacrylate was removed using twice xylene (VWR, International GmbH) for 20 min, twice 2-methoxyethylacetat for 20 min, and finally 96% ethanol. Samples were rehydrated in a graded series of ethanol in each case related to the ethanol concentration of the first staining solution. Samples were stained for light microscopy (Leica DMRBE Research Microscope, Camera Leica DC300, Leica Microsystems) as described below. Finally, sections were washed in 96% ethanol (2 min), xylene (5 min) and mounted in Canada-balsam-solution (Sigma-Aldrich Chemie GmbH) for investigation. Three histological sections of all section planes were evaluated (**Fig. 1B and C**). Presented images were taken from the central part of the 3 cm defect area.

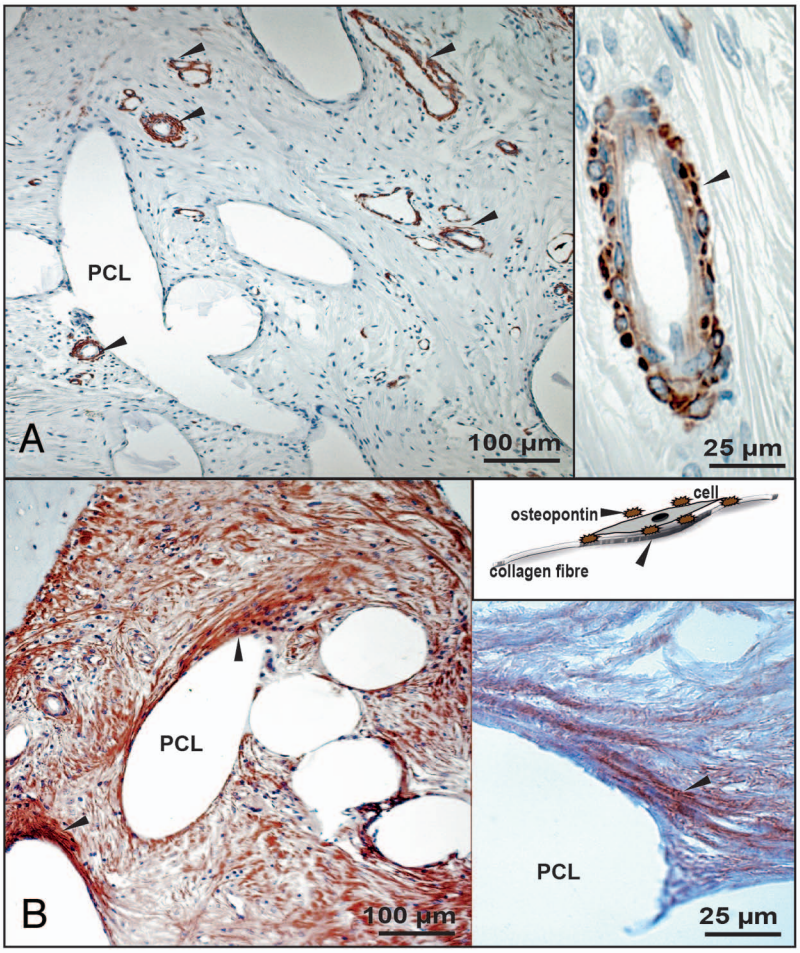

Figure 8. Anti-α smooth muscle actin and osteopontin staining: detailed investigation. (**A**) Anti- α smooth muscle actin (1A4) staining (brown), nuclei are counter stained in blue, left: general overview, vessels are marked with a black arrow; right: smooth muscle cells in vessel walls. (**B**) Osteopontin staining (brown), nuclei are counter stained in blue, black arrow marks positively stained cell-collagen-osteopontin bonds, left: general overview; right: osteopontin associated cell-collagen fiber construct, in vivo situation is schematically drawn in the upper right picture; (original magnification **A and B**, 100x).

Haematoxylin and eosin (HE) staining

The sections were incubated for 15 min in hematoxylin (according to Mayer, VWR, International GmbH), followed by a differentiation step with water for 5 min and finally stained with eosin (VWR, International GmbH) for 1 min.

Masson-Goldner trichrome staining

Nuclei were stained for 15 min with hematoxylin according to Weigert (iron-hematoxylin-Kit, VWR, International GmbH) followed by azophloxin staining for 15 min. Samples were washed in acetic acid (1%) and placed in acid orange G solution. They

were then rinsed in 1% acetic acid, for 30 s and stained with light green for 5 min, then rinsed again in 1% acetic acid for 5 min (all solutions used from Masson-Goldner trichrome staining kit, Merck KGaA).

Modified Masson-Goldner trichrome staining

Nuclei were stained for 15 min with hematoxylin according to Weigert (Weigerts iron-hematoxylin-Kit, VWR, International GmbH). Modified trichrome staining according to Masson-Goldner combines an azophloxin (15 min), orange G (5 min) and a 15 min aniline blue-tartrazine solution staining step (VWR, International GmbH). Tartrazine stains collagen structures in yellow and in combination with aniline blue which also stains collagen the final coloring results are various shades of green to yellow. Sections were washed with 3% acetic acid after each staining step.

Movat's pentachrome staining

Sections were stained with 5% sodium thiosulfate for 5 min, washed for 5 min under cold running water, stained in 1% alcian blue for 20 min and washed again. The slides were placed in pre-heated alkaline alcohol (60 °C) for 10 min, washed under running water than stained with hematoxylin according to Weigert (10 min), washed with water, then placed in Movat's solution for 60 min and washed again. Samples were stained with acid fuchsin for 1 min, differentiated in 1% acetic acid and incubated with 5% phosphotungstic acid for 5 min (Movat pentachrome stain Kit, Diapath S.p.A). The slides were transferred directly into 1% acetic acid for 5 min and washed finally.

Alcian blue staining

The sections were washed with 3% acetic acid, stained with 1% alcian blue (MORPHISTO® GmbH) for 60 min, and differentiated with 3% acetic acid. Nuclei were counter stained with 0.1% nuclear fast red solution (MORPHISTO® GmbH) for 5 min and finally washed with water.

1A4-actin and osteopontin staining

For immunohistology, 3 µm sections were incubated with the primary antibody (mouse anti human smooth muscle Actin, clone 1A4 (DAKO) or rabbit anti human osteopontin (Calbiochem, Merck Group) overnight at 4 °C, then incubated with biotin conjugated bridging antibody 1:150 in blocking solution (30 min, 37 °C) and finally incubated in avidin-biotin conjugated peroxidase (Vectastain universal Elite Kit, Vector Laboratories) for 30 min. The immune reaction was visualized with Romulin (Biocare Medical) for 15 min at room temperature. Sections were counterstained with hematoxylin according to Mayer (VWR, International GmbH) (5 min). Samples incubated without primary antibody were used as control.

Histomorphometry

The imaging software "cell^{D}" (Olympus life and material science Europa GmbH, Hamburg, Germany) was used to quantify the amount of connective tissue, PCL scaffold and new bone within the defect zone. In total 252 gray scale pictures (36 pictures per section plane) presenting the whole defect area were analyzed using defined thresholds for connective tissue, bone matrix or PCL (**Fig. 5C**). The 3 different phases were presented using a color coding function. Connective tissue is shown in green, bone matrix in yellow and PCL in red (**Fig. 5D**). Finally, the area of each threshold was measured in µm^2 per picture.

Ethical statement

The animal studies have been licensed by the regional board of Dresden (24D-9168.11-1-2006-17). All animals were cared for according to the European guidelines for the care and use of laboratory animals (Directive 24.11.1986, 86/609/CEE).

Disclosure of Potential Conflicts of Interest

No potential conflicts of interest were disclosed.

Acknowledgments

The authors thank the Catgut GmbH (Markneukirchen, Germany) and Möckel Embroidery and Engineering Company (Auerbach, Germany) for providing and producing the PCL scaffolds. They also thank A. Wenke for preparation of the histological sections. The authors thank the Sächsische Aufbaubank (SAB) for financing. W. Schneiders and S. Rammelt are funded in part by the Deutsche Forschungsgemeinschaft, DFG (TRR 67).

Author Contributions

C.R. was responsible for animal surgery, data collection, data analysis, writing, and design of data. W.S. was responsible for animal surgery and interpretation of data. S.M. performed histological preparation and staining. B.R. performed data analysis. S.R. made contributions to the conception and design of the experiments. B.R. and S.R. drafted the manuscript. All authors approved the final version of the submitted manuscript.

Supplemental Materials

Supplemental materials may be found here:
www.landesbioscience.com/journals/biomatter/article/27993

References

1. Marsell R, Einhorn TA. The biology of fracture healing. Injury 2011; 42:551-5; PMID:21489527; http://dx.doi.org/10.1016/j.injury.2011.03.031
2. Schindeler A, McDonald MM, Bokko P, Little DG. Bone remodeling during fracture repair: The cellular picture. Semin Cell Dev Biol 2008; 19:459-66; PMID:18692584; http://dx.doi.org/10.1016/j.semcdb.2008.07.004
3. Ai-Aql ZS, Alagl AS, Graves DT, Gerstenfeld LC, Einhorn TA. Molecular mechanisms controlling bone formation during fracture healing and distraction osteogenesis. J Dent Res 2008; 87:107-18; PMID:18218835; http://dx.doi.org/10.1177/154405910808700215
4. Jensen T, Jakobsen T, Baas J, Nygaard JV, Dolatshahi-Pirouz A, Hovgaard MB, Foss M, Bünger C, Besenbacher F, Søballe K. Hydroxyapatite nanoparticles in poly-D,L-lactic acid coatings on porous titanium implants conducts bone formation. J Biomed Mater Res A 2010; 95:665-72; PMID:20725972; http://dx.doi.org/10.1002/jbm.a.32863
5. Mihalko WM, Howard C, Dimaano F, Dimaano N, Hawkins M. Effects of hydroxyapatite on titanium foam as a bone ingrowth surface in acetabular shells: a canine study. J Long Term Eff Med Implants 2010; 20:35-42; PMID:21284586; http://dx.doi.org/10.1615/JLongTermEffMedImplants.v20.i1.50
6. Rammelt S, Heck C, Bernhardt R, Bierbaum S, Scharnweber D, Goebbels J, Ziegler J, Biewener A, Zwipp H. In vivo effects of coating loaded and unloaded Ti implants with collagen, chondroitin sulfate, and hydroxyapatite in the sheep tibia. J Orthop Res 2007; 25:1052-61; PMID:17457829; http://dx.doi.org/10.1002/jor.20403
7. Blokhuis TJ, Wippermann BW, den Boer FC, van Lingen A, Patka P, Bakker FC, Haarman HJ. Resorbable calcium phosphate particles as a carrier material for bone marrow in an ovine segmental defect. J Biomed Mater Res 2000; 51:369-75; PMID:10880078; http://dx.doi.org/10.1002/1097-4636(20000905)51:3<369::AID-JBM10>3.0.CO;2-J

8. Schieker M, Mutschler W. [Bridging posttraumatic bony defects. Established and new methods]. Unfallchirurg 2006; 109:715-32; PMID:16941096; http://dx.doi.org/10.1007/s00113-006-1152-z
9. Schmidt-Rohlfing B, Tzioupis C, Menzel CL, Pape HC. [Tissue engineering of bone tissue. Principles and clinical applications]. Unfallchirurg 2009; 112:785-95; PMID:19756458; http://dx.doi.org/10.1007/s00113-009-1695-x
10. Pearce AI, Richards RG, Milz S, Schneider E, Pearce SG. Animal models for implant biomaterial research in bone: a review. Eur Cell Mater 2007; 13:1-10; PMID:17334975
11. Bensaïd W, Oudina K, Viateau V, Potier E, Bousson V, Blanchat C, Sedel L, Guillemin G, Petite H. De novo reconstruction of functional bone by tissue engineering in the metatarsal sheep model. Tissue Eng 2005; 11:814-24; PMID:15998221; http://dx.doi.org/10.1089/ten.2005.11.814
12. Petite H, Viateau V, Bensaïd W, Meunier A, de Pollak C, Bourguignon M, Oudina K, Sedel L, Guillemin G. Tissue-engineered bone regeneration. Nat Biotechnol 2000; 18:959-63; PMID:10973216; http://dx.doi.org/10.1038/79449
13. Bloemers FW, Blokhuis TJ, Patka P, Bakker FC, Wippermann BW, Haarman HJ. Autologous bone versus calcium-phosphate ceramics in treatment of experimental bone defects. J Biomed Mater Res B Appl Biomater 2003; 66:526-31; PMID:12861603; http://dx.doi.org/10.1002/jbm.b.10045
14. Gugala Z, Gogolewski S. Healing of critical-size segmental bone defects in the sheep tibiae using bioresorbable polylactide membranes. Injury 2002; 33(Suppl 2):B71-6; PMID:12161322; http://dx.doi.org/10.1016/S0020-1383(02)00135-3
15. Viateau V, Guillemin G, Bousson V, Oudina K, Hannouche D, Sedel L, Logeart-Avramoglou D, Petite H. Long-bone critical-size defects treated with tissue-engineered grafts: a study on sheep. J Orthop Res 2007; 25:741-9; PMID:17318898; http://dx.doi.org/10.1002/jor.20352
16. Reichert JC, Wullschleger ME, Cipitria A, Lienau J, Cheng TK, Schütz MA, Duda GN, Nöth U, Eulert J, Hutmacher DW. Custom-made composite scaffolds for segmental defect repair in long bones. Int Orthop 2011; 35:1229-36; PMID:21136053; http://dx.doi.org/10.1007/s00264-010-1146-x
17. Blokhuis TJ, Wippermann BW, den Boer FC, van Lingen A, Patka P, Bakker FC, Haarman HJ. Resorbable calcium phosphate particles as a carrier material for bone marrow in an ovine segmental defect. J Biomed Mater Res 2000; 51:369-75; PMID:10880078; http://dx.doi.org/10.1002/1097-4636(20000905)51:3<369::AID-JBM10>3.0.CO;2-J
18. Kon E, Muraglia A, Corsi A, Bianco P, Marcacci M, Martin I, Boyde A, Ruspantini I, Chistolini P, Rocca M, et al. Autologous bone marrow stromal cells loaded onto porous hydroxyapatite ceramic accelerate bone repair in critical-size defects of sheep long bones. J Biomed Mater Res 2000; 49:328-37; PMID:10602065; http://dx.doi.org/10.1002/(SICI)1097-4636(20000305)49:3<328::AID-JBM5>3.0.CO;2-Q
19. Nuss KM, Auer JA, Boos A, von Rechenberg B. An animal model in sheep for biocompatibility testing of biomaterials in cancellous bones. BMC Musculoskelet Disord 2006; 7:67; PMID:16911787; http://dx.doi.org/10.1186/1471-2474-7-67
20. Giannoni P, Mastrogiacomo M, Alini M, Pearce SG, Corsi A, Santolini F, Muraglia A, Bianco P, Cancedda R. Regeneration of large bone defects in sheep using bone marrow stromal cells. J Tissue Eng Regen Med 2008; 2:253-62; PMID:18537203; http://dx.doi.org/10.1002/term.90
21. Sarkar MR, Augat P, Shefelbine SJ, Schorlemmer S, Huber-Lang M, Claes L, Kinzl L, Ignatius A. Bone formation in a long bone defect model using a platelet-rich plasma-loaded collagen scaffold. Biomaterials 2006; 27:1817-23; PMID:16307796; http://dx.doi.org/10.1016/j.biomaterials.2005.10.039
22. Claes L, Eckert-Hübner K, Augat P. The fracture gap size influences the local vascularization and tissue differentiation in callus healing. Langenbecks Arch Surg 2003; 388:316-22; PMID:13680236; http://dx.doi.org/10.1007/s00423-003-0396-0
23. Mastrogiacomo M, Corsi A, Francioso E, Di Comite M, Monetti F, Scaglione S, Favia A, Crovace A, Bianco P, Cancedda R. Reconstruction of extensive long bone defects in sheep using resorbable bioceramics based on silicon stabilized tricalcium phosphate. Tissue Eng 2006; 12:1261-73; PMID:16771639; http://dx.doi.org/10.1089/ten.2006.12.1261
24. Niemeyer P, Fechner K, Milz S, Richter W, Suedkamp NP, Mehlhorn AT, Pearce S, Kasten P. Comparison of mesenchymal stem cells from bone marrow and adipose tissue for bone regeneration in a critical size defect of the sheep tibia and the influence of platelet-rich plasma. Biomaterials 2010; 31:3572-9; PMID:20153047; http://dx.doi.org/10.1016/j.biomaterials.2010.01.085
25. Gao TJ, Lindholm TS, Kommonen B, Ragni P, Paronzini A, Lindholm TC, Jalovaara P, Urist MR. The use of a coral composite implant containing bone morphogenetic protein to repair a segmental tibial defect in sheep. Int Orthop 1997; 21:194-200; PMID:9266302; http://dx.doi.org/10.1007/s002640050149
26. Marcacci M, Kon E, Zaffagnini S, Giardino R, Rocca M, Corsi A, Benvenuti A, Bianco P, Quarto R, Martin I, et al. Reconstruction of extensive long-bone defects in sheep using porous hydroxyapatite sponges. Calcif Tissue Int 1999; 64:83-90; PMID:9868289; http://dx.doi.org/10.1007/s002239900583
27. Reichert JC, Cipitria A, Epari DR, Saifzadeh S, Krishnakanth P, Berner A, Woodruff MA, Schell H, Mehta M, Schuetz MA, et al. A tissue engineering solution for segmental defect regeneration in load-bearing long bones. Sci Transl Med 2012; 4:141ra93; PMID:22764209; http://dx.doi.org/10.1126/scitranslmed.3003720
28. Harms C, Helms K, Taschner T, Stratos I, Ignatius A, Gerber T, Lenz S, Rammelt S, Vollmar B, Mittlmeier T. Osteogenic capacity of nanocrystalline bone cement in a weight-bearing defect at the ovine tibial metaphysis. Int J Nanomedicine 2012; 7:2883-9; PMID:22745551; http://dx.doi.org/10.2147/IJN.S29314
29. Lohfeld S, Cahill S, Barron V, McHugh P, Dürselen L, Kreja L, Bausewein C, Ignatius A. Fabrication, mechanical and in vivo performance of polycaprolactone/tricalcium phosphate composite scaffolds. Acta Biomater 2012; 8:3446-56; PMID:22652444; http://dx.doi.org/10.1016/j.actbio.2012.05.018
30. Liu T, Wu G, Wismeijer D, Gu Z, Liu Y. Deproteinized bovine bone functionalized with the slow delivery of BMP-2 for the repair of critical-sized bone defects in sheep. Bone 2013; 56:110-8; PMID:23732874; http://dx.doi.org/10.1016/j.bone.2013.05.017
31. Rammelt S, Corbeil D, Manthey S, Zwipp H, Hanisch U. Immunohistochemical in situ characterization of orthopedic implants on polymethyl metacrylate embedded cutting and grinding sections. J Biomed Mater Res A 2007; 83:313-22; PMID:17437302; http://dx.doi.org/10.1002/jbm.a.31243
32. Rentsch B, Hofmann A, Breier A, Rentsch C, Scharnweber D. Embroidered and surface modified polycaprolactone-co-lactide scaffolds as bone substitute: in vitro characterization. Ann Biomed Eng 2009; 37:2118-28; PMID:19626441; http://dx.doi.org/10.1007/s10439-009-9731-0
33. Rentsch C, Schneiders W, Hess R, Rentsch B, Bernhardt R, Spekl K, Schneider K, Scharnweber D, Biewener A, Rammelt S. Healing properties of surface-coated polycaprolactone-co-lactide scaffolds: A pilot study in sheep. J Biomater Appl 2014; 28:654-66; PMID:23413230; http://dx.doi.org/10.1177/0885328212471409